

Article

In Silico Studies on Selected Neutral Molecules, CGa_2Ge_2 , CAIGaGe_2 , and CSiGa_2Ge Containing Planar Tetracoordinate Carbon

Prasenjit Das ¹  and Pratim Kumar Chattaraj ^{1,2,*} 

¹ Department of Chemistry, Indian Institute of Technology Kharagpur, Kharagpur 721302, India; pdas2305@iitkgp.ac.in

² Department of Chemistry, Indian Institute of Technology Bombay, Mumbai 400076, India

* Correspondence: pkc@chem.iitkgp.ac.in

Abstract: Density functional theory (DFT) was used to study the structure, stability, and bonding in some selected neutral pentaatomic systems, *viz.*, CGa_2Ge_2 , CAIGaGe_2 , and CSiGa_2Ge containing planar tetracoordinate carbon. The systems are kinetically stable, as predicted from the ab initio molecular dynamics simulations. The natural bond orbital (NBO) analysis showed that strong electron donation occurs to the central planar carbon atom by the peripheral atoms in all the studied systems. From the nucleus independent chemical shift (NICS) analysis, it is shown that the systems possess both σ - and π - aromaticity. The presence of 18 valence electrons in these systems, in their neutral form, appears to be important for their stability with planar geometries rather than tetrahedral structures. The nature of bonding is understood through the adaptive natural density partitioning analysis (AdNDP), quantum theory of atoms in molecules (QTAIM) analysis, and also via Wiberg bond index (WBI) and electron localization function (ELF).

Keywords: planar tetracoordinate carbon; σ/π aromaticity; ab initio molecular dynamics simulations; neutral 18 valence electrons complexes; Wiberg bond index (WBI)



Citation: Das, P.; Chattaraj, P.K. In *Silico Studies on Selected Neutral Molecules, CGa_2Ge_2 , CAIGaGe_2 , and CSiGa_2Ge Containing Planar Tetracoordinate Carbon*. *Atoms* **2021**, *9*, 65. <https://doi.org/10.3390/atoms9030065>

Academic Editors: Venkatesan S. Thimmakonda and Krishnan Thirumorthy

Received: 4 August 2021

Accepted: 7 September 2021

Published: 10 September 2021

Publisher's Note: MDPI stays neutral with regard to jurisdictional claims in published maps and institutional affiliations.



Copyright: © 2021 by the authors. Licensee MDPI, Basel, Switzerland. This article is an open access article distributed under the terms and conditions of the Creative Commons Attribution (CC BY) license (<https://creativecommons.org/licenses/by/4.0/>).

1. Introduction

Nowadays, planar tetracoordinate carbon (ptC) molecules showed great attention to experimentalists [1–7] as well as theoreticians [8–15] because it deviates from the usual ideas of tetrahedral tetracoordinate carbon. The tetrahedral carbon concept was given by van't Hoff and Le Bel in 1874 [16,17]. The idea of the ptC was introduced in 1968 by H. J. Monkhorst as a transition state of methane in a non-dissociative racemization process [18]. After two years, Hoffmann and co-workers showed two strategies for the stabilization of molecules containing ptC and those methods constitute a useful guide to design new ptC molecules [8,19]. The first one is the electronic strategy that involves appropriate substituents with σ -donors and π -acceptors simultaneously to stabilize the ptC species. The second one is the mechanical strategy that involves aromatic systems, cages, and transition metals to design and stabilize ptC systems. Using those two proposals, Schleyer and co-workers, in 1976, designed lithium substituted cyclopropane ($\text{C}_3\text{H}_3\text{Li}_2$), the first in-silico studied ptC molecule [9]. After that, many theoretical studies from different research groups were reported on ptC systems [12,20–27]. In a theoretical work in 1991, Schleyer and Boldyrev proposed *cis* and *trans* geometries of CSi_2Al_2 molecules containing ptC [28]. In order to understand the stability of the ptC systems, the “18 valence electron rule” was composed and many systems were shown to obey this rule [2]. However, there are some examples in which more or less than 18 valence electrons are present and the ptC systems are still stable [29,30]. One of the most recent theoretical work shows that the CAI_4Mg system in its neutral and mono-anionic state show global minima with ptC [30]. The neutral ptC system shows 18 valence electrons and the anionic one possesses 19 valence electrons.

Despite their *in silico* characterization, experimental synthesis and characterization of ptC molecules are limited [1–7]. In 1999, CAI_4^- , a pentaatomic monoanionic cluster, was identified in the gas phase [1]. After one year, some new anionic ptC molecules, CAI_4^{2-} , CAI_3Ge^- , CAI_3Si^- , and NaCAI_4^- , were experimentally detected [7,31,32]. More interestingly, this idea of ptC has been extended to design planar pentacoordinate [33–35] and hexacoordinate carbon molecules [36–39].

Boldyrev and Simons [2] studied on three neutral pentaatomic molecules (CSi_2Al_2 , CSi_2Ga_2 , and CGe_2Al_2) and showed the planar tetracoordinate central carbon (ptC) in these systems. They used molecular orbital analysis to rationalize the preference of the planar geometry over the tetrahedral one and they concluded that molecules containing one central C and two Si or Ge ligand atoms and two Al or Ga ligand atoms should have stable planar geometries. Inspired by this work, we designed three neutral pentaatomic systems, *viz.*, CGa_2Ge_2 , CALGaGe_2 , and CSiGa_2Ge , containing 18 valence electrons. Both *cis* and *trans* isomers of the systems are considered in this present work. The electronic interaction among the middle carbon atom and the peripheral atoms is responsible for the planar arrangement of these molecules obeying the “electronic strategy method” for their stabilization. All these three systems follow the 18 valence electrons rule to gain stability in planar form. With the help of the DFT method, we studied the geometries, stability, and the nature of bonding in the molecules. Now, the nature of bonding includes molecular orbital analysis, AdNDP analysis, NBO analysis, and electron density analysis.

2. Computational Details

The geometry optimization and the subsequent frequency calculation of all the systems considered in this study were carried out using BP86 functional [40,41] coupled with D3 correction [42]. The BP86 functional is one of the commonly used DFT methods for electronic structure calculations for main group elements. The correlation consistent triple- ζ quality basis set has been taken for this computation. For C, Al, and Si atoms cc-pVTZ basis set and for Ga and Ge atoms cc-pVTZ-PP basis set along with relativistic effective core potential (RECPs), ECP10MDF have been used [43–46]. All real harmonic vibrational frequencies correspond to the energy minima on the potential energy surfaces, as observed. Using the same computational method the aromaticity analysis of the studied ptC systems was performed, with the help of NICS. All of these computations were performed with the help of the Gaussian 16 program package [47].

The atom-centered density matrix propagation (ADMP) simulation [48–50] for the studied systems was performed to obtain information about their kinetic stability at 300 K and 500 K temperatures, and 1 atm pressure over 2000 fs of simulation time. The simulation was performed with the BP86-D3/def2-SVP method by taking the initially optimized geometries.

To know about the charge distribution in the systems and the Wiberg bond indices (WBI) [51] between any two atoms connected through a bond, natural bond orbital (NBO) [52] analysis was performed using NBO 3.1 [52,53] as implemented in Gaussian 16, using the same computational method that was used for the geometry optimization.

The atoms-in-molecules (AIM) [54] analysis was carried out at the same level that was used for the geometry optimization, using the Multiwfn program package [55]. We have generated various bond critical points (BCPs) and also analyzed the ELF basin [56].

3. Results and Discussion

3.1. Geometries

The optimized geometries of the cyclic rings (L) and the ptC systems, both in *cis* and *trans* orientations, are given in Figure 1. The L and ptC systems were optimized without any symmetry constraint. In this work, we considered only the singlet state of the ptC systems because the higher spin states correspond to a higher energy than the singlet state. Moreover, the mono-anionic and mono-cationic states of these ptC systems are not planar. So, we considered only neutral states of the studied systems. For all L systems, *cis* isomers

of AlGaGe₂ and SiGa₂Ge rings have C_s symmetry and the *cis* Ga₂Ge₂ ring has C_{2v} symmetry. For AlGaGe₂ and SiGa₂Ge rings, the *trans* isomers correspond to the C_{2v} point group of symmetry while, for the Ga₂Ge₂ ring, the *trans* isomer has D_{2h} symmetry. The carbon atom at the middle of the rings bonded with four peripheral atoms of each L and the ptC systems were generated. We took the tetrahedral structures of the systems as an initial guess but, after optimization, the structures are converted to more stable planar forms. The energy differences between *cis* and *trans* isomers are 2.45, 3.70, and 1.50 kcal/mol for CGa₂Ge₂, CAIGaGe₂, and CSiGa₂Ge systems, respectively. At the second-order Møller–Plesset perturbation (MP2) method [57] with the same basis set, the energy differences are 1.40, 2.27, and 0.72 kcal/mol for CGa₂Ge₂, CAIGaGe₂, and CSiGa₂Ge systems, respectively. So, we considered both isomers throughout the work. The *trans* isomer of the CGa₂Ge₂ system has D_{2h} point group of symmetry while the *trans* isomers of CAIGaGe₂ and CSiGa₂Ge systems have C_{2v} point group. However, the *cis* isomers of CAIGaGe₂ and CSiGa₂Ge systems have C_s symmetry, and the *cis* CGa₂Ge₂ system has C_{2v} symmetry. The bond distances for all the bonds in the systems are presented in Figure 1. Boldyrev and Simons [2] explained that tetrahedral structures of their systems are Jahn–Teller unstable and subsequent distortion should lead to a planar structure. For this purpose, they compared the occupancy pattern of the valence MOs of tetrahedral CF₄ molecule with the tetrahedral structures of their systems. The CF₄ molecule is the 32 valence electronic system and the occupancy pattern of the occupied MOs is 1a₁²1t₂⁶2a₁²2t₂⁶1e⁴3t₂⁶1t₁⁶. They assumed that other tetrahedral molecules or nearly tetrahedral structures would follow this occupancy pattern (except for symmetry-imposed degeneracies) and that the 18 valence electronic tetrahedral structures showed a 1a₁²1t₂⁶2a₁²2t₂⁶1e² pattern of occupancy. Due to this partially filled e orbital, the tetrahedral structures of their systems show Jahn–Teller instability and obtain distorted to a planar structure.

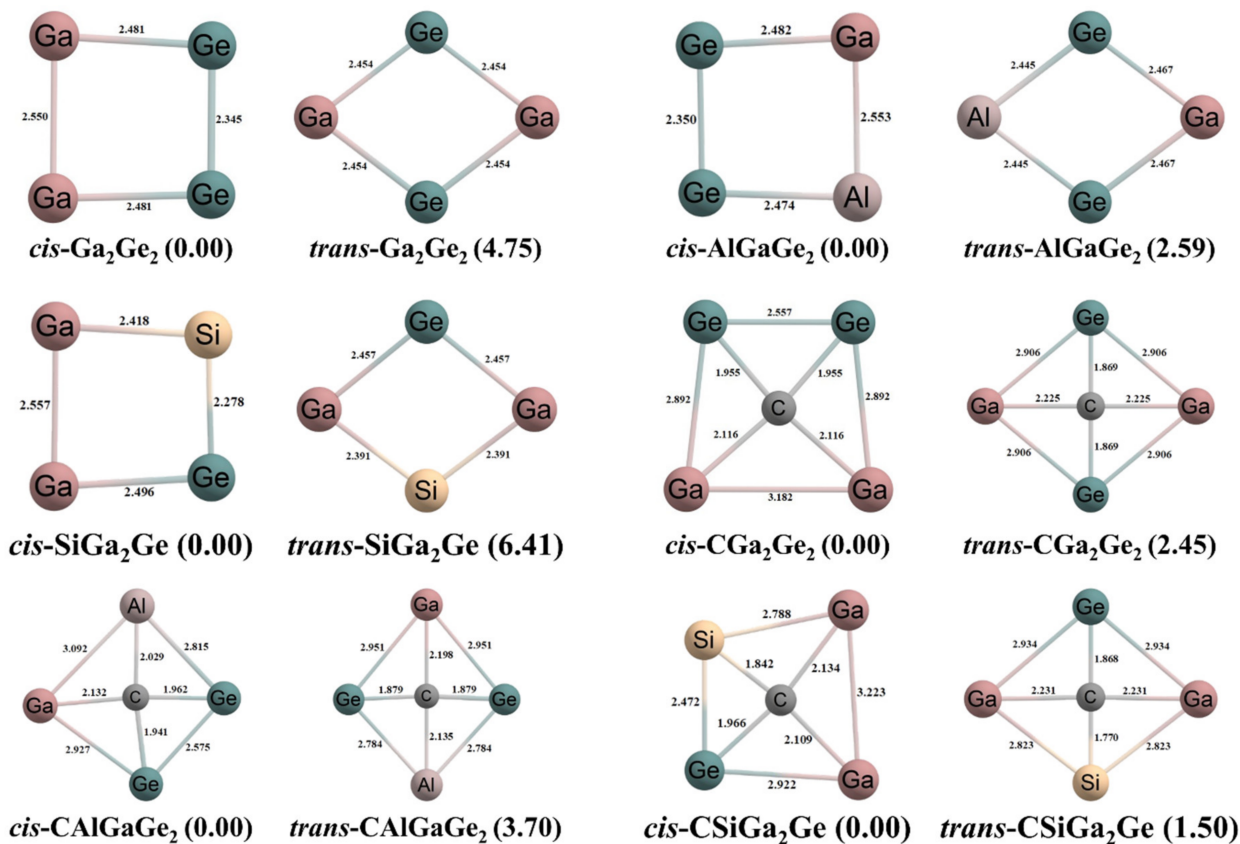


Figure 1. The optimized geometries of the cyclic rings and the ptC systems. Bond lengths are given in Å unit. The values in the parentheses are the relative energies in kcal/mol. The energies of *cis* isomers are considered to be zero.

Our designed systems are very similar to the systems studied by Boldyrev and Simons. The systems have 18 valence electrons and the carbon atom is present at the central position. So, our systems in tetrahedral structures also show a similar occupancy pattern of the occupied MOs and that is $1a_1^2 1t_2^6 2a_1^2 2t_2^6 1e^2$. Due to this partially filled e orbital the tetrahedral structures of our designed systems show Jahn-Teller instability and distorted to a planar structure. So, considering Jahn–Teller distortion the ground state of our systems show planar geometries.

Ab initio molecular dynamics simulations were performed at 300 K and 500 K temperatures and 1 atm pressure over 2000 fs of time to check the kinetic stability for both isomers using ADMP approach. The time evolution of energy of all the systems is presented in Figure 2. The oscillation in the plots arises because of the increase in the nuclear kinetic energy during structural deformation throughout the whole simulation. Some snapshots at different time steps of the simulation for *cis* and *trans* isomers are given in Figures 3 and 4, respectively, to show the structural deformation of these systems at these temperatures. The steady fluctuations in energy and consistency in the geometry suggest the kinetic stability of these systems both in *cis* and *trans* isomers at these temperatures.

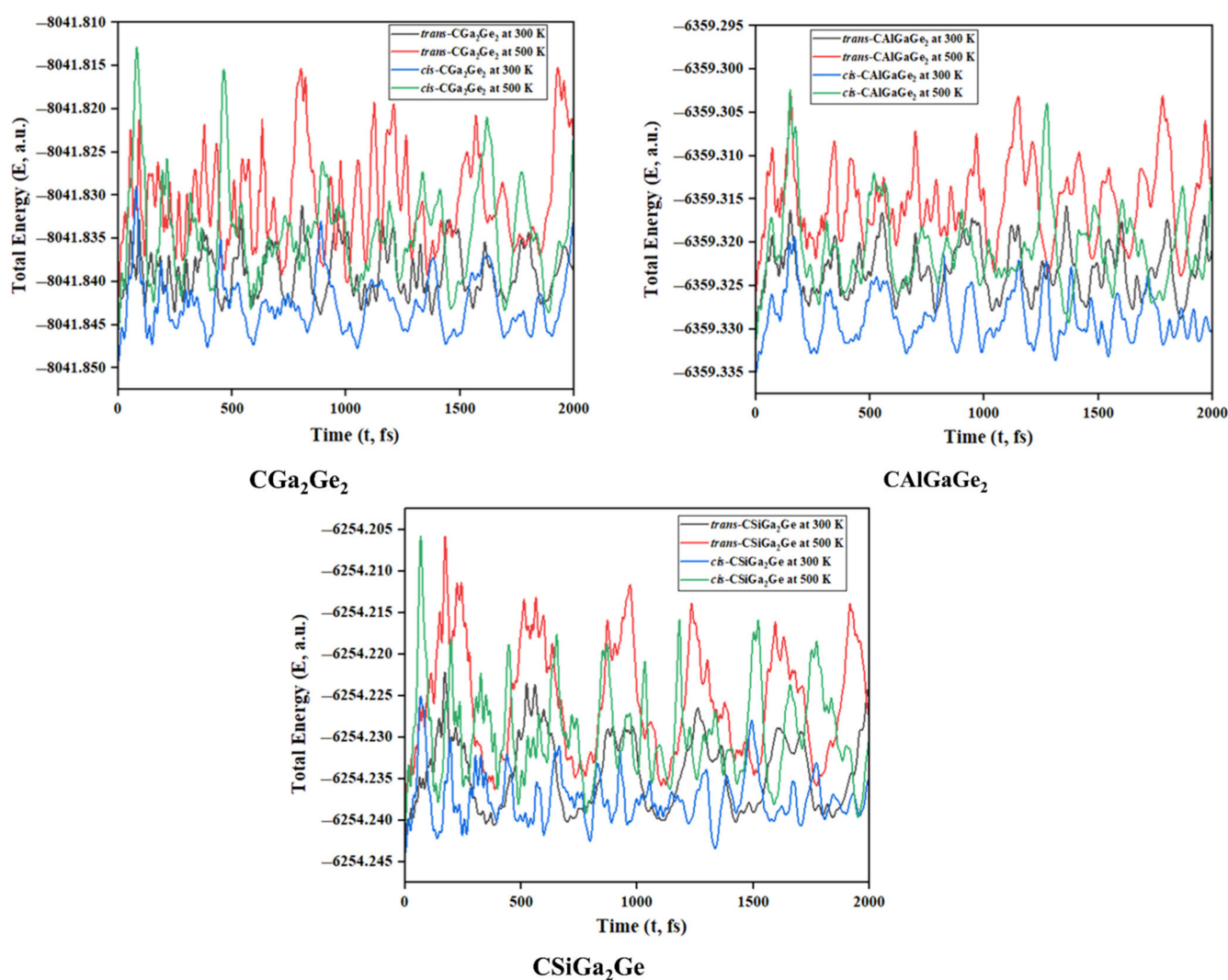


Figure 2. Time evolution of total energy for CGa_2Ge_2 , CAIGaGe_2 , and CSiGa_2Ge systems, respectively.

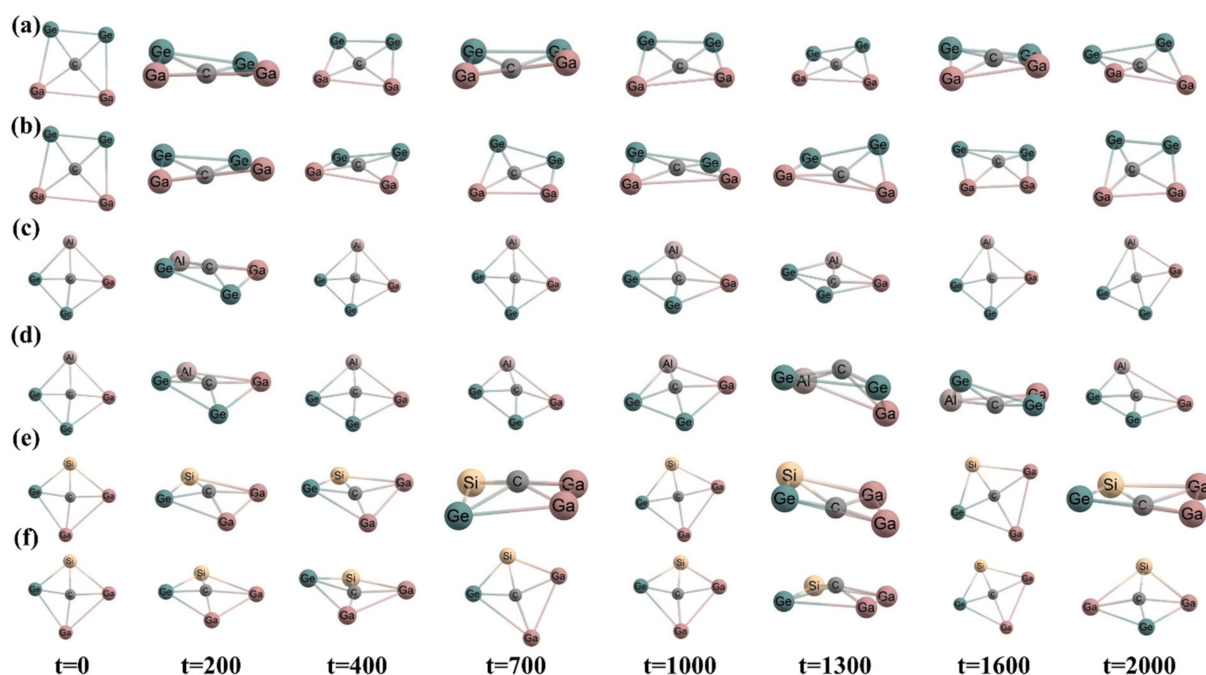


Figure 3. Snapshots at different time steps (time in fs) (a,c,e) at 300 K temperature and (b,d,f) at 500 K temperature of CGa₂Ge₂, AlGaGe₂, and CSiGa₂Ge systems, respectively, in *cis* geometry.

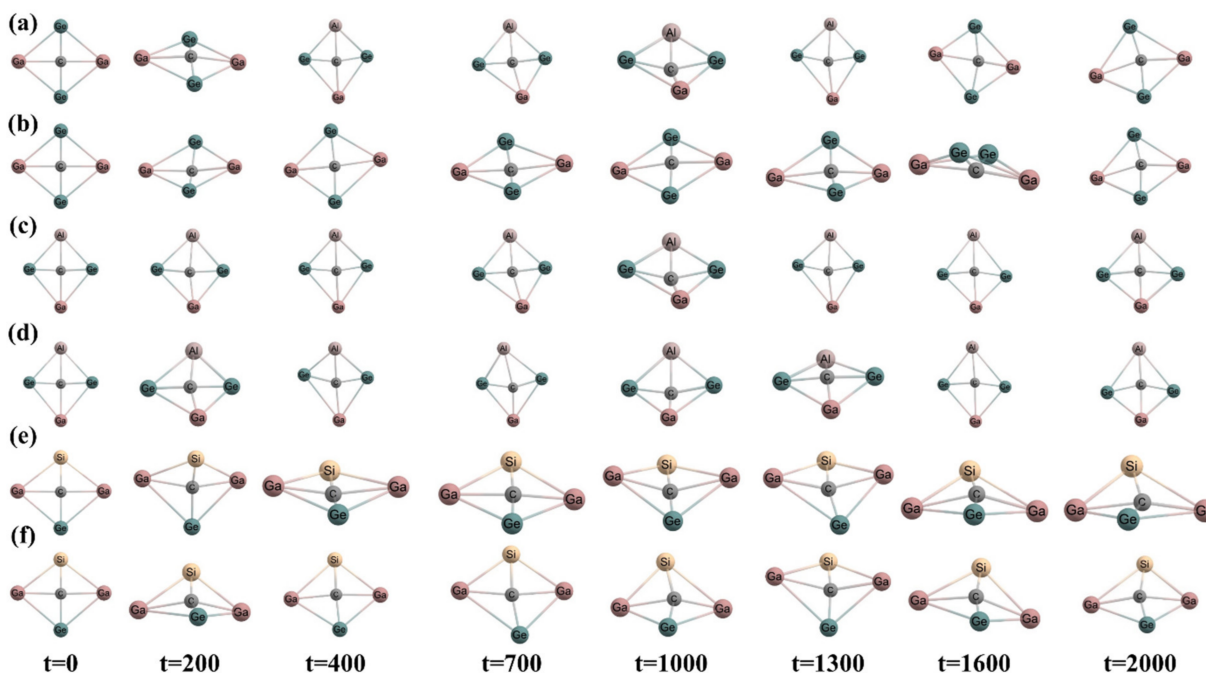


Figure 4. Snapshots at different time steps (time in fs) (a,c,e) at 300 K temperature and (b,d,f) at 500 K temperature of CGa₂Ge₂, AlGaGe₂, and CSiGa₂Ge systems, respectively, in *trans* geometry.

3.2. Molecular Orbitals

The molecular orbital analysis for the systems was carried out to obtain more information about the bonding. The molecular orbitals along with associated energies for all the systems in *cis* and *trans* isomers are presented in Figure 5. The lowest unoccupied molecular orbitals (LUMOs) are the π -type orbitals distributed over the four membered rings. The HOMO-3 molecular orbitals in the systems are π -type molecular orbitals and are delocalized over the whole molecule. In the HOMO-3 π -delocalized MO of the systems, significant contribution comes from the perpendicular $2p_z$ orbital and $2p_x$ orbital of central

ptC in *cis* and *trans* isomers, respectively. This σ - and π - delocalization of electron density support the electronic stabilization in the designed ptC systems. We discussed the electronic delocalization within the systems based on multi-center-2e bonding in the AdNDP section in detail. The highest occupied molecular orbital (HOMO), HOMO-1 and HOMO-2 orbitals, are σ -type molecular orbitals. The energy differences (ΔE_{H-L}) between the HOMO and the LUMO are 1.99, 1.80, 1.97 eV, and 1.26, 0.98, 1.28 eV, for *cis* and *trans* isomers for CGa_2Ge_2 , CAIGaGe_2 , and CSiGa_2Ge systems, respectively. The *cis* isomers showed higher ΔE_{H-L} values than that of the *trans* isomers indicating greater stability [58–60].

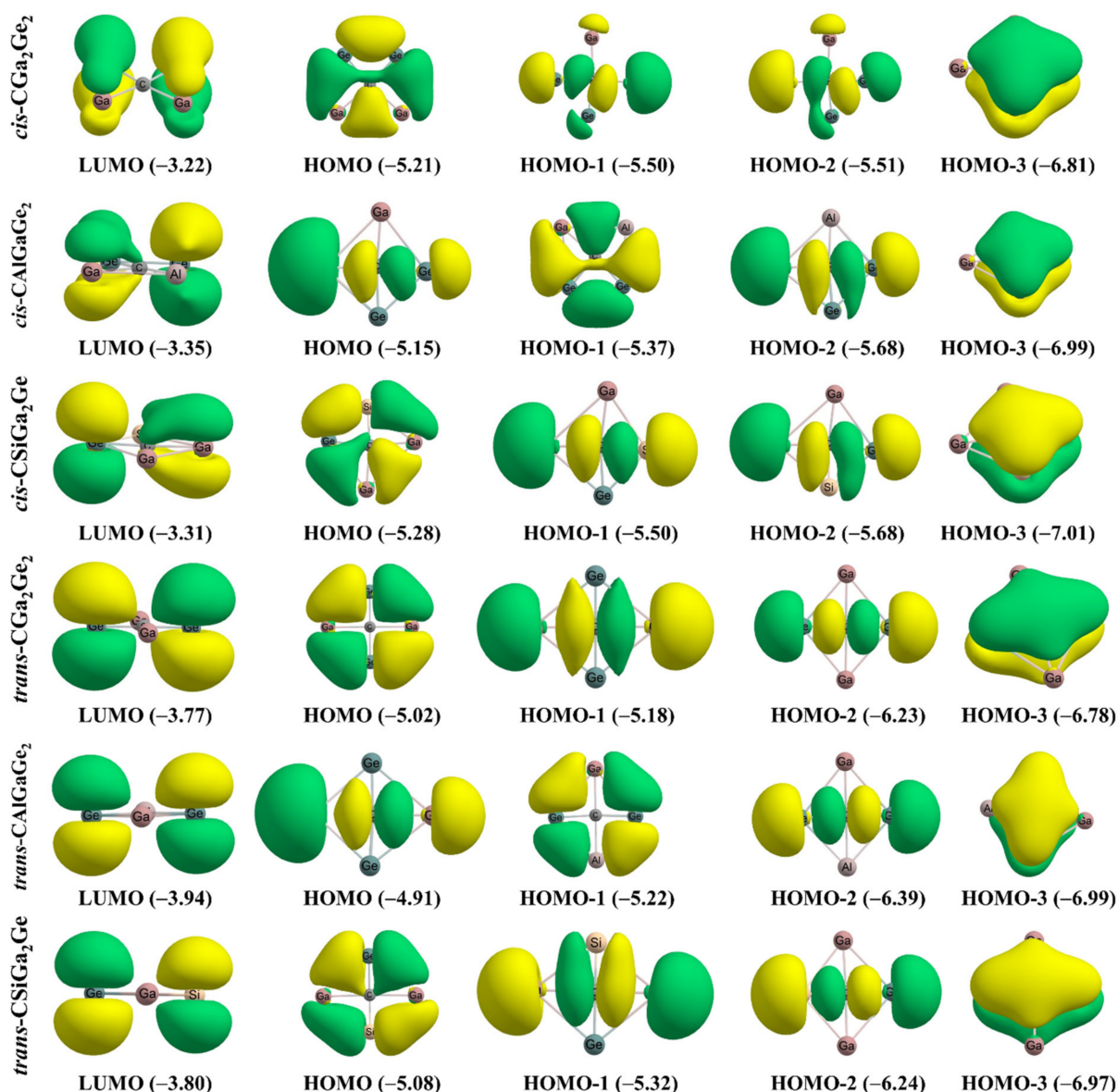


Figure 5. Plots of the molecular orbitals of the systems. The values in the parenthesis are the energies of the corresponding orbitals in the eV unit.

3.3. Natural Bond Orbital (NBO) Analysis

The distribution of natural charge in the studied ptC molecules and the WBI values for a bond was analyzed using the natural bond orbital scheme. This analysis showed that a significant amount of charge transfer occurred from the peripheral atoms to the central carbon atom and the C atom is highly negative in each ptC system. The values of the natural charges on the atoms are shown in Table 1. The natural charges on central C atoms vary from $-2.14 |e|$ to $-2.23 |e|$ in the ptC systems and the peripheral atoms

show positive charges. The AlGaGe_2 system showed the highest negative charges and the CGa_2Ge_2 system showed the lowest negative charges on the central C atom, respectively. The charges on C atoms in the ptC systems are the same or almost the same in both *cis* and *trans* isomers but the charges on the peripheral atoms are different for the two isomers. The valence electronic configurations of C atoms in the systems are presented in Table 1. It is well known that, in ptC systems, the central C atoms act as both a σ -acceptor and a π -donor. In our present study, the σ -acceptor is evident from the highly negative charge on C centers in all the systems (see Table 1). From the valence electronic configuration of C centers as shown in Table 1, in the case of *cis* isomers, the population of $2p_z$ orbital is lower than that of the $2p_x$ and $2p_y$ orbitals, and, in *trans* isomers the population of $2p_x$ orbital is lower than that of the $2p_y$ and $2p_z$ orbitals of all the ptC systems. These lower populations of $2p_z$ and $2p_x$ orbitals for *cis* and *trans* isomers, respectively, is a consequence of π -donation from the central carbon atom [34]. The *cis* isomers of the systems lie on the XY plane and the *trans* isomers of the systems lie on the YZ plane. The valence p orbitals along these perpendicular axes, i.e., the $2p_z$ orbital and $2p_x$ orbital of central carbon atom in the *cis* and *trans* isomers of the systems, respectively, take part in delocalized π -bonding. The WBI values for C–Al, C–Si, C–Ga, and C–Ge bonds were computed for both isomers of all the ptC systems, and the numerical values are presented in Table 2. The WBI values for the C–Si bonds are 1.09 and 1.18 for *cis* and *trans* isomers of CSiGa_2Ge system, indicating pure covalent bonds. Similarly for C–Ge bonds, the WBI values are in the range of 0.99 to 1.04 for *cis* isomers and 1.09 to 1.13 for *trans* isomers of the systems. These $\text{WBI}_{\text{C-Ge}}$ values indicate the covalent nature of the bonds. The WBI values for C–Al and C–Ga bonds are comparatively lower than that of the C–Si and C–Ge bonds, indicating the partial covalent character of these bonds. The WBI values for the C–Ga bonds are comparable with that reported in the theoretical study by Zhou et al. [61]. The WBI values for the C–Si and C–Ge bonds in *trans* isomers are a little bit higher than that in the *cis* isomers. However, for C–Al and C–Ga bonds, the WBI values in *cis* isomers are a little bit higher than those in the *trans*-isomers.

Table 1. The natural charges (q , $|e|$) on the atoms in the rings and the ptC systems and the valence electronic configuration of C atom in the ptC systems.

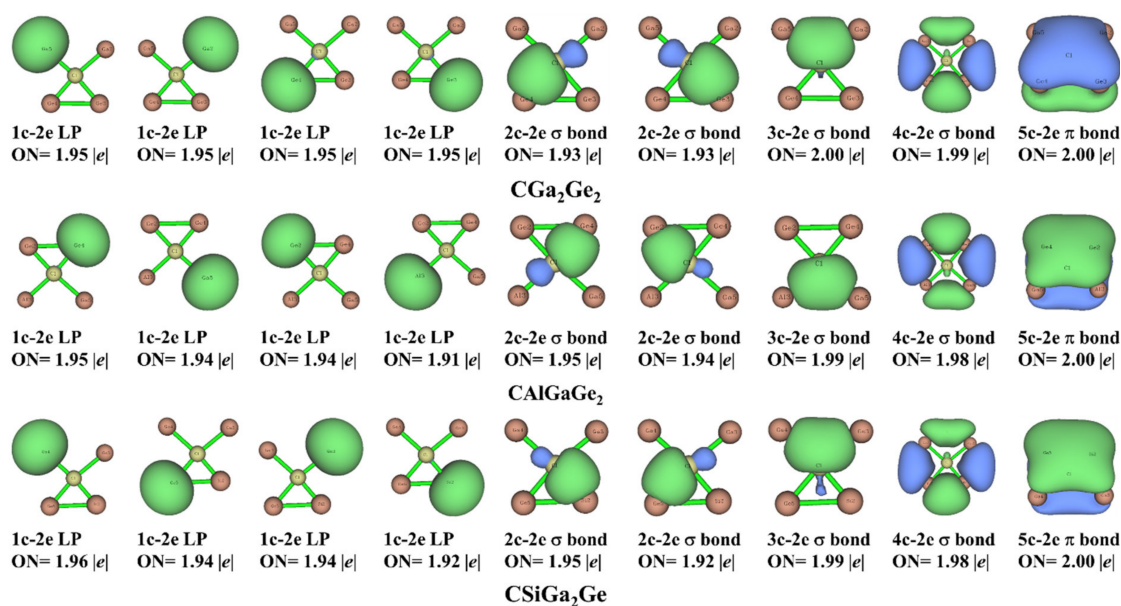
Systems	q_{C}	q_{Al}	q_{Si}	q_{Ga}	q_{Ge}	Valence Electronic Configuration of C
<i>cis</i> - Ga_2Ge_2	-	-	-	0.32 0.32	-0.32 -0.32	-
<i>trans</i> - Ga_2Ge_2	-	-	-	0.21 0.21	-0.21 -0.21	-
<i>cis</i> - CGa_2Ge_2	-2.14	-	-	0.59 0.59	0.49 0.49	$2s^{1.606} 2p_x^{1.583} 2p_y^{1.598} 2p_z^{1.315}$
<i>trans</i> - CGa_2Ge_2	-2.14	-	-	0.50 0.50	0.58 0.58	$2s^{1.548} 2p_x^{1.408} 2p_y^{1.552} 2p_z^{1.596}$
<i>cis</i> - AlGaGe_2	-	0.47	-	0.36	-0.42 -0.42	-
<i>trans</i> - AlGaGe_2	-	0.33	-	0.15	-0.17 -0.30	-
<i>cis</i> - AlGaGe_2	-2.22	0.64	-	0.59	0.48 0.51	$2s^{1.612} 2p_x^{1.593} 2p_y^{1.638} 2p_z^{1.341}$
<i>trans</i> - AlGaGe_2	-2.23	0.55	-	0.54	0.57 0.57	$2s^{1.556} 2p_x^{1.412} 2p_y^{1.555} 2p_z^{1.661}$
<i>cis</i> - SiGa_2Ge	-	-	-0.41	0.34 0.34	-0.27	-
<i>trans</i> - SiGa_2Ge	-	-	-0.28	0.22 0.25	-0.19	-
<i>cis</i> - CSiGa_2Ge	-2.16	-	0.47	0.59 0.60	0.51	$2s^{1.590} 2p_x^{1.581} 2p_y^{1.635} 2p_z^{1.312}$
<i>trans</i> - CSiGa_2Ge	-2.18	-	0.58	0.51 0.51	0.59	$2s^{1.528} 2p_x^{1.421} 2p_y^{1.590} 2p_z^{1.593}$

Table 2. Wiberg bond indices (WBI) for some selected bonds in the ptC molecules.

Complexes	WBI (C–Al)	WBI (C–Si)	WBI (C–Ga)	WBI (C–Ge)
<i>cis</i> -CGa ₂ Ge ₂	-	-	0.37	1.04
			0.37	1.04
<i>trans</i> -CGa ₂ Ge ₂	-	-	0.31	1.13
			0.31	1.13
<i>cis</i> -CAIGaGe ₂	0.33	-	0.34	1.02
			1.03	1.09
<i>trans</i> -CAIGaGe ₂	0.30	-	0.31	1.09
			1.09	1.09
<i>cis</i> -CSiGa ₂ Ge	-	1.09	0.34	0.99
			0.36	0.99
<i>trans</i> -CSiGa ₂ Ge	-	1.18	0.29	1.09
			0.29	1.09

3.4. Adaptive Natural Density Partitioning (AdNDP) Analysis

We carried out AdNDP analysis [62,63] in bonding context for both *cis* and *trans* isomers of the studied systems. We used this technique to investigate the presence of *n*-center-two-electron (*nc*-2e) bonds (*n* ranges from 1 (lone pair) to the maximum number of atoms (completely delocalized bonding)). Figures 6 and 7 represent the results from this analysis for *cis* and *trans* isomers, respectively. The results showed the appearance of four lone pairs (1-center-two-electron bonds) on the four peripheral atoms and the occupation numbers (ON) are in between 1.91–1.96 |*e*| and 1.90–1.96 |*e*| in *cis* and *trans* isomers, respectively. There are two 2-center-two-electron (2c-2e) σ bonds in both isomers of the systems. Additionally, one 3-center-two-electron (3c-2e) σ bond, one 4-center-two-electron (4c-2e) σ bond, and one 5-center-two-electron (5c-2e) π -bond in *cis* isomers; and one 4-center-two-electron (4c-2e) σ bond, one 5-center-two-electron (5c-2e) σ bond, and one 5-center-two-electron (5c-2e) π -bond in *trans* isomers are present for all the systems. The occupation numbers of these *nc*-2e bonds in the systems under consideration are presented in Figures 6 and 7 for *cis* and *trans* isomers, respectively. This analysis shows that in the designed ptC systems the central carbon atom is present in the $2\pi/6\sigma$ framework. Thus, the $2\pi/6\sigma$ frameworks and peripheral 4c-2e σ bonds are crucial for the stability of these ptC species. Both the σ - and π - delocalization of electron densities supported the stability of the designed system in planar form.

**Figure 6.** AdNDP bonding patterns of the systems in *cis* isomer with the occupation numbers (ONs).

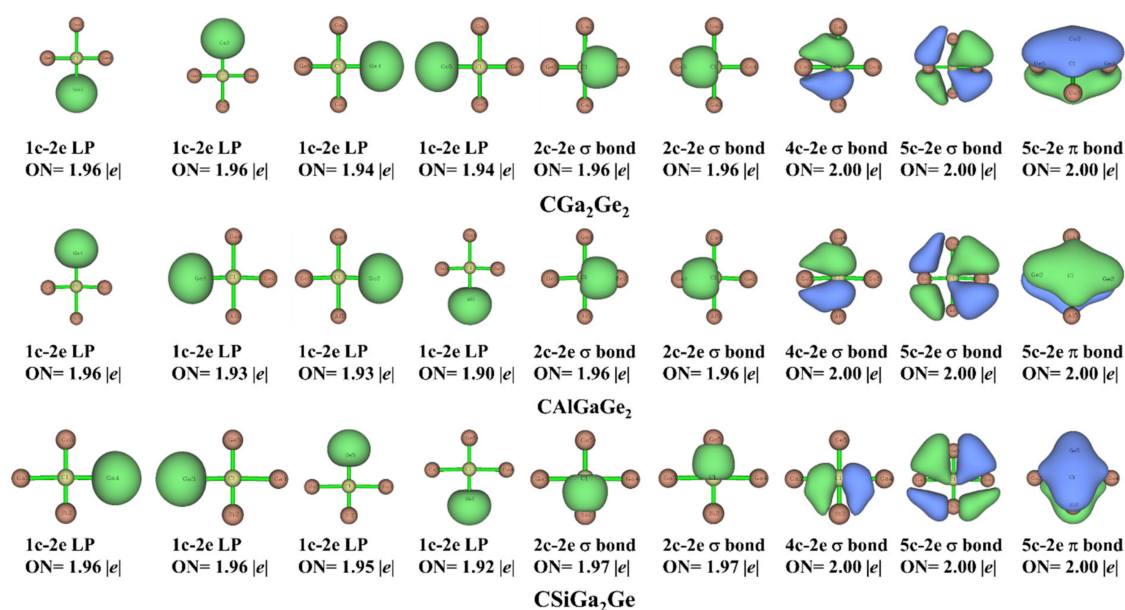


Figure 7. AdNDP bonding patterns of the systems in *trans* isomer with the occupation numbers (ONs).

3.5. Atoms in Molecule (AIM) Analysis

We generated various electron density descriptors at all the $(3, -1)$ bond critical points (BCPs) of the studied systems, and the numerical values are shown in Table 3. The contour plots of $\nabla^2\rho(r)$ along the bond paths for the systems are presented in Figure 8. From the presented BCPs in Table 3, the existence of bonds between the middle carbon atom (C) and the four peripheral atoms is confirmed in all the systems. The low $\rho(r_c)$ values and positive $\nabla^2\rho(r_c)$ values suggest that there is a closed-shell type of bonding. From the negative values of $H(r_c)$ at the corresponding BCPs, it may be argued that the bonds have a partial covalent character. The values of $-G(r_c)/V(r_c)$ at different BCPs are between 0.5 and 1.0, indicating the absence of a noncovalent interaction.

Table 3. Electron Density ($\rho(r_c)$), Laplacian of Electron Density ($\nabla^2\rho(r_c)$), Kinetic Energy Density ($G(r_c)$), Potential Energy Density ($V(r_c)$), Total Energy Density ($H(r_c)$) for the ptC systems.

Complexes	BCP	$\rho(r_c)$	$\nabla^2\rho(r_c)$	$G(r_c)$	$V(r_c)$	$H(r_c)$	ELF	$-G(r_c)/V(r_c)$	$G(r_c)/\rho(r_c)$
<i>cis</i> -CGa ₂ Ge ₂	C-Ga	0.078	0.131	0.060	-0.088	-0.028	0.311	0.682	0.769
	C-Ge	0.115	0.139	0.092	-0.148	-0.057	0.420	0.622	0.800
<i>trans</i> -CGa ₂ Ge ₂	C-Ga	0.063	0.098	0.044	-0.063	-0.019	0.295	0.698	0.698
	C-Ge	0.134	0.207	0.124	-0.196	-0.072	0.399	0.633	0.925
<i>cis</i> -CAlGaGe ₂	C-Al	0.064	0.224	0.072	-0.088	-0.016	0.224	0.818	1.125
	C-Ga	0.075	0.125	0.057	-0.083	-0.026	0.125	0.687	0.760
<i>trans</i> -CAlGaGe ₂	C-Ge	0.112	0.137	0.089	-0.144	-0.055	0.417	0.618	0.795
	C-Al	0.053	0.152	0.052	-0.065	-0.014	0.149	0.800	0.981
<i>cis</i> -CSiGa ₂ Ge	C-Ga	0.067	0.103	0.047	-0.069	-0.022	0.308	0.681	0.701
	C-Ge	0.131	0.198	0.119	-0.188	-0.069	0.399	0.633	0.908
	C-Si	0.112	0.284	0.136	-0.201	-0.065	0.233	0.677	1.214
<i>trans</i> -CSiGa ₂ Ge	C-Ga	0.074	0.126	0.057	-0.082	-0.025	0.305	0.695	0.770
	C-Ge	0.111	0.139	0.088	-0.142	-0.054	0.139	0.620	0.793
	C-Si	0.126	0.415	0.175	-0.246	-0.071	0.211	0.711	1.389
<i>trans</i> -CSiGa ₂ Ge	C-Ga	0.061	0.099	0.043	-0.062	-0.018	0.287	0.694	0.705
	C-Ge	0.135	0.209	0.126	-0.199	-0.073	0.400	0.633	0.933

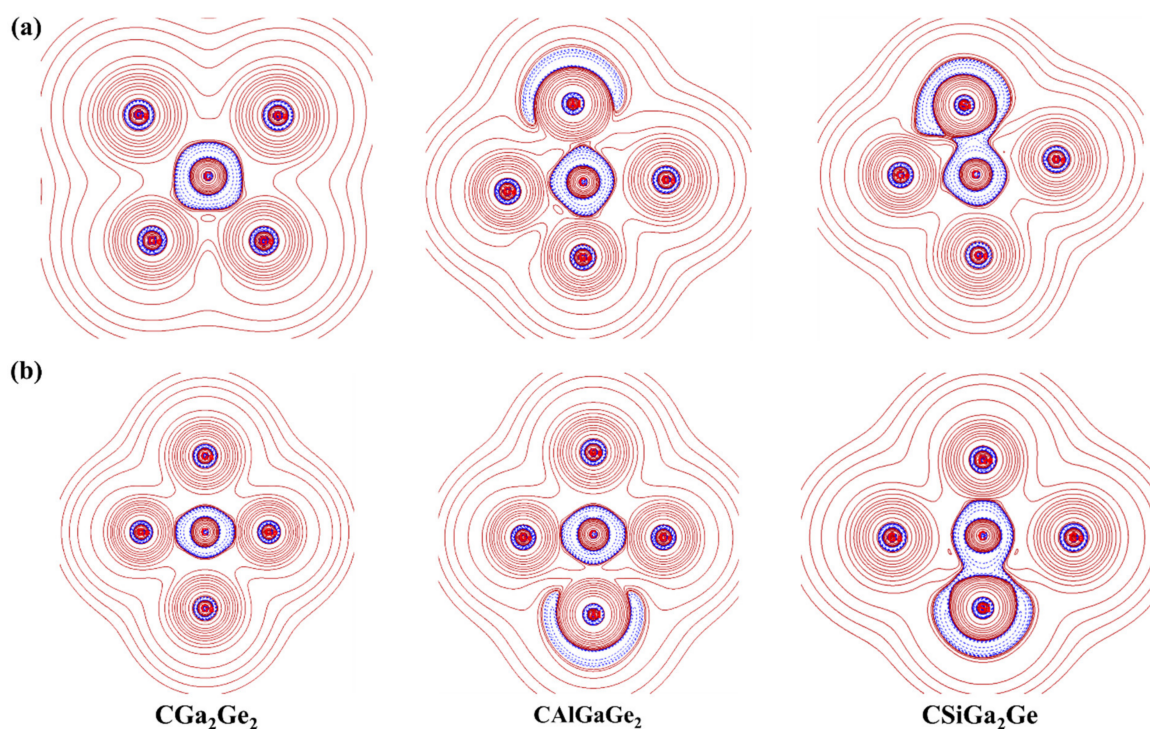


Figure 8. The plots of the Laplacian of electron density [$\nabla^2\rho(r)$], blue dashed and red solid lines indicate $\nabla^2\rho(r) < 0$ and $\nabla^2\rho(r) > 0$ regions, respectively, for (a) *cis* isomer; (b) *trans* isomer, for CGa_2Ge_2 , CAIGaGe_2 , and CSiGa_2Ge systems.

The ELF plots for both the isomers of the systems were generated, and the plots are presented in Figure 9. The ELF plots show the interaction among the middle C atom and the peripheral atoms and the electron densities are delocalized within the whole molecule. These ELF plots are in support of stability of the systems in planar geometries in terms of electron delocalization within the ptC systems.

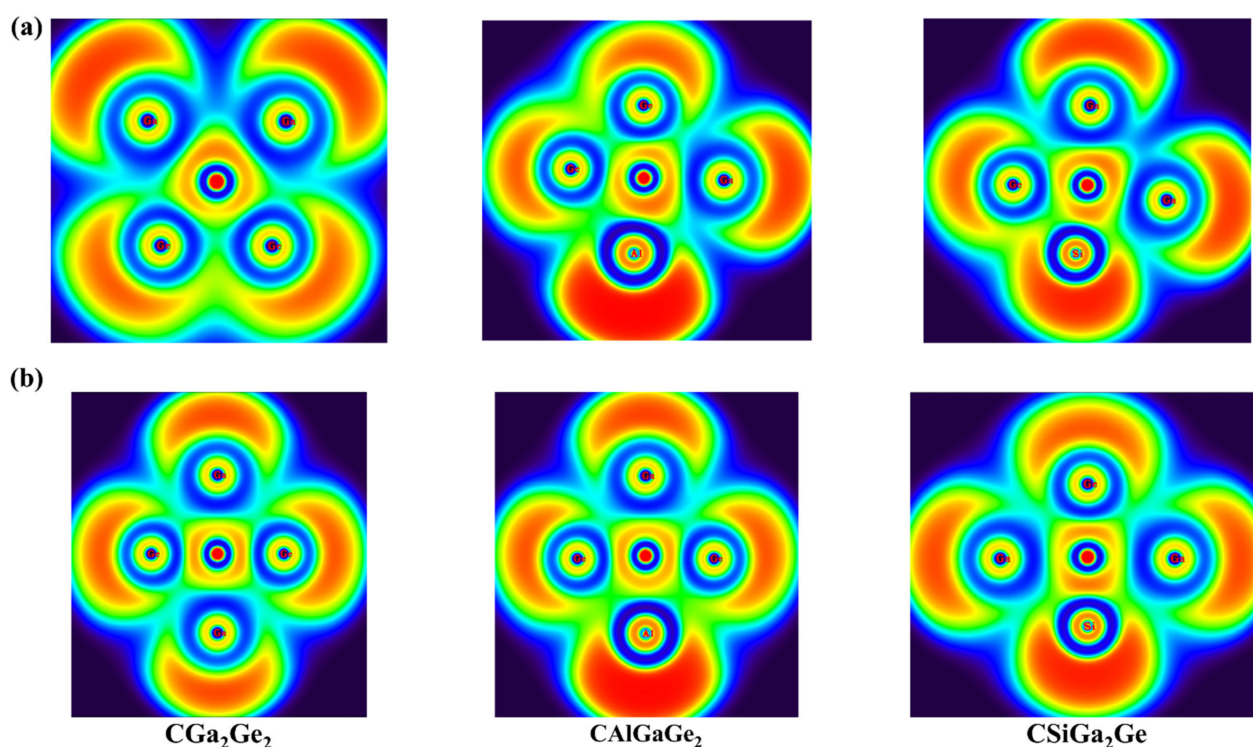


Figure 9. The color-filled plots of the electron localization function (ELF) basin for (a) *cis* isomer; (b) *trans* isomer, for CGa_2Ge_2 , CAIGaGe_2 , and CSiGa_2Ge systems.

3.6. Aromaticity Analysis

Aromatic molecules are cyclic, planar, conjugated, and have $(4n + 2)$ π electrons. To predict the aromaticity of molecules, NICS is an efficient criterion proposed by Schleyer and co-workers [64,65]. NICS is calculated based on the use of magnetic shielding tensor for a dummy magnetic dipole considered at the center of an under-examination ring. It is called a nucleus-independent chemical shift, because there is no nucleus at the center of the molecular ring to experience the effective magnetic field. Molecules are considered aromatic based on the negative NICS values, and the positive NICS values indicate anti-aromatic systems. The non-aromatic systems have NICS values close to zero.

We computed both NICS(0) and NICS(1) at the middle of each triangle by placing a ghost atom at the plane and 1 Å above the plane. We also computed NICS(1) of the four membered ring by placing the ghost atom at 1 Å above the central C atom for all the systems for *cis* and *trans* isomers. The results of this analysis are presented in Figure 10. Both the NICS(0) and NICS(1) values for each triangle and the NICS(1) values at 1 Å above the central C atom of the ring are negative. These negative values of NICS(0) and NICS(1) are the indicators of σ - and π - aromaticity, albeit approximately. In aromatic systems, the electron densities are delocalized throughout the molecule. In all of our designed systems, the electron density is delocalized, as shown from the molecular orbitals, ELF plots, and the multi-center-2e-bonds of all the systems. So, these computed negative NICS values support the stability of the designed ptC systems.

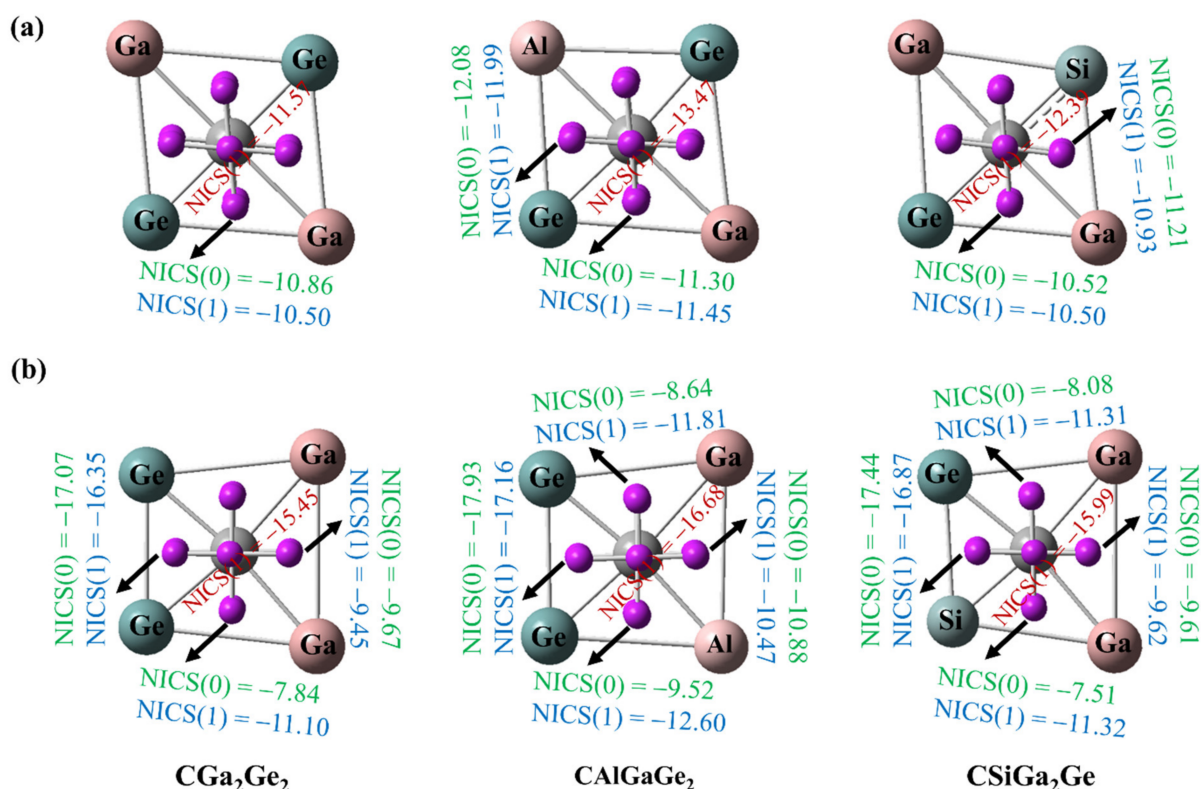


Figure 10. Nucleus independent chemical shifts (NICSs; in ppm) for (a) *trans* geometries; (b) *cis* geometries. The values in the red color indicate the NICS (1) values at 1 Å above the central C atom of the ring.

4. Summary and Conclusions

The three neutral ptC systems considered in this work possess 18 valence electrons and show stability in planar form. The stability of both *cis* and *trans* isomers of these systems is reported in this work. The NICS calculations showed that the systems possess both σ - and π - aromaticities that support the stability of the designed systems. The ADMP simulation at 300 K and 500 K temperatures over 2000 fs of time revealed the kinetic stability of the

molecules. The AIM analysis suggested the presence of bonds between the central C atom and the four peripheral atoms. We believe that this theoretical study will help in designing new ptC molecules.

Experimentally ptC systems were characterized in the gas phase. It is also our hope that the designed ptC systems could be interesting to the experimentalists. Considering all the supported results for the planar geometries of these studied systems, the experimental realization of these ptC systems could be possible in the gas phase or matrix isolation. In isolation, the systems may exist in planar form. When the systems are interacting with other species, the structures of the systems may or may not be planar; however, if the bound species create sufficient steric forces, the systems may exist in planar form.

Author Contributions: Conceptualization, P.D.; methodology, P.D. and P.K.C.; software, P.D.; validation, P.D. and P.K.C.; formal analysis, P.D.; investigation, P.K.C.; resources, P.K.C.; data curation, P.D.; writing—original draft preparation, P.D.; writing—review and editing, P.K.C.; visualization, P.D. and P.K.C.; supervision, P.K.C.; project administration, P.K.C. All authors have read and agreed to the published version of the manuscript.

Funding: DST, New Delhi, India for the J. C. Bose National Fellowship, grant number SR/S2/JCB-09/2009.

Institutional Review Board Statement: Not applicable.

Informed Consent Statement: Not applicable.

Data Availability Statement: Data available in article.

Acknowledgments: PKC thanks DST, New Delhi, India for the J. C. Bose National Fellowship. PD thanks UGC, New Delhi, India for the Research Fellowship.

Conflicts of Interest: The authors declare that they have no conflict of interests regarding the publication of this article, financial, and/or otherwise.

References

1. Li, X.; Wang, L.S.; Boldyrev, A.I.; Simons, J. Tetracoordinated Planar Carbon in the Al_4C^- Anion. A Combined Photoelectron Spectroscopy and ab Initio Study. *J. Am. Chem. Soc.* **1999**, *121*, 6033–6038. [[CrossRef](#)]
2. Boldyrev, A.I.; Simons, J. Tetracoordinated Planar Carbon in Pentaatomic Molecules. *J. Am. Chem. Soc.* **1998**, *120*, 7967–7972. [[CrossRef](#)]
3. Röttger, D.; Erker, G. Compounds Containing Planar-Tetracoordinate Carbon. *Angew. Chem. Int. Ed. Engl.* **1997**, *36*, 812–827. [[CrossRef](#)]
4. Erker, G. Planar-Tetracoordinate Carbon: Making Stable Anti-van't Hoff/Le Bel Compounds. *Comment. Inorg. Chem.* **1992**, *13*, 111–131. [[CrossRef](#)]
5. Keese, R. Carbon Flatland: Planar Tetracoordinate Carbon and Fenestranes. *Chem. Rev.* **2006**, *106*, 4787–4808. [[CrossRef](#)]
6. Xu, J.; Zhang, X.; Yu, S.; Ding, Y.H.; Bowen, K.H. Identifying the Hydrogenated Planar Tetracoordinate Carbon: A Combined Experimental and Theoretical Study of CAI_4H and CAI_4H^- . *J. Phys. Chem. Lett.* **2017**, *8*, 2263–2267. [[CrossRef](#)]
7. Li, X.; Zhang, H.F.; Wang, L.S.; Geske, G.; Boldyrev, A. Pentaatomic Tetracoordinate Planar Carbon, $[CAI_4]^{2-}$: A New Structural Unit and Its Salt Complexes. *Angew. Chem. Int. Ed.* **2000**, *39*, 3630–3632. [[CrossRef](#)]
8. Hoffmann, R.; Alder, R.W.; Wilcox, C.F. Planar Tetracoordinate Carbon. *J. Am. Chem. Soc.* **1970**, *92*, 4992–4993. [[CrossRef](#)]
9. Collins, J.B.; Dill, J.D.; Jemmis, E.D.; Apeloig, Y.; von Ragué Schleyer, P.; Seeger, R.; Pople, J.A. Stabilization of Planar Tetracoordinate Carbon. *J. Am. Chem. Soc.* **1976**, *98*, 5419–5427. [[CrossRef](#)]
10. Merino, G.; Méndez-Rojas, M.A.; Beltrán, H.I.; Corminboeuf, C.; Heine, T.; Vela, A. Theoretical Analysis of the Smallest Carbon Cluster Containing a Planar Tetracoordinate Carbon. *J. Am. Chem. Soc.* **2004**, *126*, 16160–16169. [[CrossRef](#)]
11. Yang, L.M.; Ganz, E.; Chen, Z.; Wang, Z.X.; von Ragué Schleyer, P. Four Decades of the Chemistry of Planar Hypercoordinate Compounds. *Angew. Chem. Int. Ed.* **2015**, *54*, 9468–9501. [[CrossRef](#)]
12. Thirumorthy, K.; Thimmakonda, V.S. Flat Crown Ethers with Planar Tetracoordinate Carbon Atoms. *Int. J. Quantum Chem.* **2021**, *121*, e26479. [[CrossRef](#)]
13. Yañez, O.; Vásquez-Espinal, A.; Báez-Grez, R.; Rabanal-León, W.A.; Osorio, E.; Ruiz, L.; Tiznado, W. Carbon Rings Decorated with Group 14 Elements: New Aromatic Clusters Containing Planar Tetracoordinate Carbon. *New J. Chem.* **2019**, *43*, 6781–6785. [[CrossRef](#)]
14. Thirumorthy, K.; Karton, A.; Thimmakonda, V.S. From High-Energy C_7H_2 Isomers with A Planar Tetracoordinate Carbon Atom to an Experimentally Known Carbene. *J. Phys. Chem. A* **2018**, *122*, 9054–9064. [[CrossRef](#)]

15. Suresh, C.H.; Frenking, G. Direct 1-3 Metal-Carbon Bonding and Planar Tetracoordinated Carbon in Group 6 Metallacyclobutadienes. *Organometallics* **2010**, *29*, 4766–4769. [[CrossRef](#)]
16. van't Hoff, J.H. A Suggestion Looking to the Extension into Space of the Structural Formulas at Present Used in Chemistry, and a Note upon the Relation between the Optical Activity and the Chemical Constitution of Organic Compounds. *Arch. Neerl. Sci. Exactes Nat.* **1874**, *9*, 445–454.
17. Le-Bel, J.A. On the Relations Which Exist between the Atomic Formulas of Organic Compounds and the Rotatory Power of Their Solutions. *Bull. Soc. Chim. Fr.* **1874**, *22*, 337–347.
18. Monkhorst, H.J. Activation Energy for Interconversion of Enantiomers Containing an Asymmetric Carbon Atom without Breaking Bonds. *Chem. Commun.* **1968**, *11*, 1111–1112. [[CrossRef](#)]
19. Hoffmann, R. The theoretical design of novel stabilized systems. *Pure Appl. Chem.* **1971**, *28*, 181–194. [[CrossRef](#)]
20. Sateesh, B.; Srinivas Reddy, A.; Narahari Sastry, G. Towards Design of the Smallest Planar Tetracoordinate Carbon and Boron Systems. *J. Comput. Chem.* **2007**, *28*, 335–343. [[CrossRef](#)] [[PubMed](#)]
21. Job, N.; Karton, A.; Thirumoorthy, K.; Cooksy, A.L.; Thimmakonda, V.S. Theoretical Studies of SiC₄H₂ Isomers Delineate Three Low-Lying Silylidenes are Missing in the Laboratory. *J. Phys. Chem. A* **2020**, *124*, 987–1002. [[CrossRef](#)] [[PubMed](#)]
22. Guo, J.C.; Feng, L.Y.; Dong, C.; Zhai, H.J. Ternary 12-electron CBe₃X₃⁺ (X = H, Li, Na, Cu, Ag) Clusters: Planar Tetracoordinate Carbons and Superalkali Cations. *Phys. Chem. Chem. Phys.* **2019**, *21*, 22048–22056. [[CrossRef](#)]
23. Nandula, A.; Trinh, Q.T.; Saeys, M.; Alexandrova, A.N. Origin of Extraordinary Stability of Square-Planar Carbon Atoms in Surface Carbides of Cobalt and Nickel. *Angew. Chem. Int. Ed.* **2015**, *54*, 5312–5316. [[CrossRef](#)]
24. Cui, Z.H.; Contreras, M.; Ding, Y.H.; Merino, G. Planar Tetracoordinate Carbon versus Planar Tetracoordinate Boron: The Case of CB₄ and Its Cation. *J. Am. Chem. Soc.* **2011**, *133*, 13228–13231. [[CrossRef](#)]
25. Thirumoorthy, K.; Cooksy, A.; Thimmakonda, V.S. Si₂C₅H₂ Isomers—Search Algorithms Versus Chemical Intuition. *Phys. Chem. Chem. Phys.* **2020**, *22*, 5865–5872. [[CrossRef](#)] [[PubMed](#)]
26. Jimenez-Halla, J.O.C.; Wu, Y.B.; Wang, Z.X.; Islas, R.; Heine, T.; Merino, G. CA₄Be and CA₃Be₂[−]: Global Minima with a Planar Pentacoordinate Carbon Atom. *Chem. Commun.* **2010**, *46*, 8776–8778. [[CrossRef](#)] [[PubMed](#)]
27. Cui, Z.H.; Ding, Y.H.; Cabellos, J.L.; Osorio, E.; Islas, R.; Restrepo, A.; Merino, G. Planar tetracoordinate carbons with a double bond in CA₃E clusters. *Phys. Chem. Chem. Phys.* **2015**, *17*, 8769–8775. [[CrossRef](#)] [[PubMed](#)]
28. von Ragué Schleyer, P.; Boldyrev, A.I. A new, general strategy for achieving planar tetracoordinate geometries for carbon and other second row periodic elements. *J. Chem. Soc. Chem. Commun.* **1991**, *21*, 1536–1538. [[CrossRef](#)]
29. Wu, X.-F.; Cheng, Y.-X.; Guo, J.-C. CLiAl₂E and CLi₂AlE (E = P, As, Sb, Bi): Planar Tetracoordinate Carbon Clusters with 16 and 14 Valence Electrons. *ACS Omega* **2019**, *4*, 21311–21318. [[CrossRef](#)] [[PubMed](#)]
30. Job, N.; Khatun, M.; Thirumoorthy, K.; CH, S.S.R.; Chandrasekaran, V.; Anoop, A.; Thimmakonda, V.S. CA₄Mg^{0/−}: Global Minima with a Planar Tetracoordinate Carbon Atom. *Atoms* **2021**, *9*, 24. [[CrossRef](#)]
31. Wang, L.-S.; Boldyrev, A.I.; Li, X.; Simons, J. Experimental Observation of Pentaatomic Tetracoordinate Planar Carbon-Containing Molecules. *J. Am. Chem. Soc.* **2000**, *122*, 7681–7687. [[CrossRef](#)]
32. Boldyrev, A.I.; Wang, L.-S. Beyond Classical Stoichiometry: Experiment and Theory. *J. Phys. Chem. A* **2001**, *105*, 10759–10775. [[CrossRef](#)]
33. Pei, Y.; An, W.; Ito, K.; von Ragué Schleyer, P.; Zeng, X.C. Planar Pentacoordinate Carbon in CA₅⁺: A Global Minimum. *J. Am. Chem. Soc.* **2008**, *130*, 10394–10400. [[CrossRef](#)] [[PubMed](#)]
34. Pan, S.; Cabellos, J.L.; Orozco, M.; Merino, G.; Zhao, L.; Chattaraj, P.K. Planar Pentacoordinate Carbon in CGa₅⁺ Derivatives. *Phys. Chem. Chem. Phys.* **2018**, *20*, 12350–12355. [[CrossRef](#)] [[PubMed](#)]
35. Vassilev-Galindo, V.; Pan, S.; Donald, J.K.; Merino, G. Planar Pentacoordinate Carbons. *Nat. Chem. Rev.* **2018**, *2*, 0114. [[CrossRef](#)]
36. Exner, K.; von Ragué Schleyer, P. Planar Hexacoordinate Carbon: A Viable Possibility. *Science* **2000**, *290*, 1937–1940. [[CrossRef](#)]
37. Averkiev, B.B.; Zubarev, D.Y.; Wang, L.M.; Huang, W.; Wang, L.S.; Boldyrev, A.I. Carbon Avoids Hypercoordination in CB₆[−], CB₆^{2−}, and C₂B₅[−] Planar Carbon-Boron Clusters. *J. Am. Chem. Soc.* **2008**, *130*, 9248–9250. [[CrossRef](#)]
38. Ito, K.; Chen, Z.; Corminboeuf, C.; Wannere, C.S.; Zhang, X.H.; Li, Q.S.; von Ragué Schleyer, P. Myriad Planar Hexacoordinate Carbon Molecules Inviting Synthesis. *J. Am. Chem. Soc.* **2007**, *129*, 1510–1511. [[CrossRef](#)]
39. Zhang, C.F.; Han, S.J.; Wu, Y.B.; Lu, H.G.; Lu, G. Thermodynamic Stability versus Kinetic Stability: Is the Planar Hexacoordinate Carbon Species D_{3h} CN₃Mg₃⁺ Viable? *J. Phys. Chem. A* **2014**, *118*, 3319–3325. [[CrossRef](#)] [[PubMed](#)]
40. Perdew, J.P. Density-functional approximation for the correlation energy of the inhomogeneous electron gas. *Phys. Rev. B* **1986**, *33*, 8822. [[CrossRef](#)]
41. Becke, A.D. Density-functional exchange-energy approximation with correct asymptotic behavior. *Phys. Rev. A* **1988**, *38*, 3098. [[CrossRef](#)] [[PubMed](#)]
42. Grimme, S.; Antony, J.; Ehrlich, S.; Krieg, H. A consistent and accurate ab initio parametrization of density functional dispersion correction (DFT-D) for the 94 elements H-Pu. *J. Chem. Phys.* **2010**, *132*, 154104. [[CrossRef](#)] [[PubMed](#)]
43. Dunning, T.H., Jr. Gaussian basis sets for use in correlated molecular calculations. I. The atoms boron through neon and hydrogen. *J. Chem. Phys.* **1989**, *90*, 1007–1023. [[CrossRef](#)]
44. Kendall, R.A.; Dunning, T.H., Jr.; Harrison, R.J. Electron affinities of the first-row atoms revisited. Systematic basis sets and wave functions. *J. Chem. Phys.* **1992**, *96*, 6796–6806. [[CrossRef](#)]

45. Metz, B.; Stoll, H.; Dolg, M. Small-core multiconfiguration-Dirac-Hartree-Fock-adjusted pseudopotentials for post-d main group elements: Application to PbH and PbO. *J. Chem. Phys.* **2000**, *113*, 2563–2569. [[CrossRef](#)]
46. Peterson, K.A. Systematically convergent basis sets with relativistic pseudopotentials. I. Correlation consistent basis sets for the post-d group 13–15 elements. *J. Chem. Phys.* **2003**, *119*, 11099–11112. [[CrossRef](#)]
47. Frisch, M.J.; Trucks, G.W.; Schlegel, H.B.; Scuseria, G.E.; Robb, M.A.; Cheeseman, J.R.; Scalmani, G.; Barone, V.; Petersson, G.A.; Nakatsuji, H.; et al. *Gaussian 16 Revision B.01*; Gaussian Inc.: Wallingford, CT, USA, 2016.
48. Schlegel, H.B.; Millam, J.M.; Iyengar, S.S.; Voth, G.A.; Daniels, A.D.; Scuseria, G.E.; Frisch, M.J. Ab initio molecular dynamics: Propagating the density matrix with Gaussian orbitals. *J. Chem. Phys.* **2001**, *114*, 9758–9763. [[CrossRef](#)]
49. Iyengar, S.S.; Schlegel, H.B.; Millam, J.M.; Voth, G.A.; Scuseria, G.E.; Frisch, M.J. Ab initio molecular dynamics: Propagating the density matrix with Gaussian orbitals. II. Generalizations based on mass-weighting, idempotency, energy conservation and choice of initial conditions. *J. Chem. Phys.* **2001**, *115*, 10291–10302. [[CrossRef](#)]
50. Schlegel, H.B.; Iyengar, S.S.; Li, X.; Millam, J.M.; Voth, G.A.; Scuseria, G.E.; Frisch, M.J. Ab initio molecular dynamics: Propagating the density matrix with Gaussian orbitals. III. Comparison with Born-Oppenheimer dynamics. *J. Chem. Phys.* **2002**, *117*, 8694–8704. [[CrossRef](#)]
51. Wiberg, K.B. Application of the pople-santry-segal CNDO method to the cyclopropylcarbanyl and cyclobutyl cation and to bicyclobutane. *Tetrahedron* **1968**, *24*, 1083–1096. [[CrossRef](#)]
52. Reed, A.E.; Curtiss, L.A.; Weinhold, F. Intermolecular interactions from a natural bond orbital, donor-acceptor viewpoint. *Chem. Rev.* **1988**, *88*, 899–926. [[CrossRef](#)]
53. Glendenning, E.D.; Reed, A.E.; Carpenter, J.E.; Weinhold, F. *NBO 3.1 QCPE Bulletin*. 1990, Volume 10, p. 58. Available online: [https://www.scirp.org/\(S\(czeh2tfqw2orz553k1w0r45\)\)/reference/referencespapers.aspx?referenceid=1595007](https://www.scirp.org/(S(czeh2tfqw2orz553k1w0r45))/reference/referencespapers.aspx?referenceid=1595007) (accessed on 1 August 2021).
54. Bader, R.F.W. Atoms in Molecules. In *A Quantum Theory*; Oxford University Press: Oxford, UK, 1990.
55. Lu, T.; Chen, F. Multiwfn: A multifunctional wavefunction analyzer. *J. Comput. Chem.* **2012**, *33*, 580–592. [[CrossRef](#)]
56. Becke, A.D.; Edgecombe, K.E. A simple measure of electron localization in atomic and molecular systems. *J. Chem. Phys.* **1990**, *92*, 5397. [[CrossRef](#)]
57. Møller, C.; Plesset, M.S. Note on an Approximation Treatment for Many Electron Systems. *Phys. Rev.* **1934**, *46*, 618–622. [[CrossRef](#)]
58. Parr, R.G.; Chattaraj, P.K. Principle of maximum hardness. *J. Am. Chem. Soc.* **1991**, *113*, 1854–1855. [[CrossRef](#)]
59. Chattaraj, P.K.; Cedillo, A.; Parr, R.G.; Arnett, E.M. Appraisal of Chemical Bond Making, Bond Breaking, and Electron Transfer in Solution in the Light of the Principle of Maximum Hardness. *J. Org. Chem.* **1995**, *60*, 4707–4714. [[CrossRef](#)]
60. Chakraborty, D.; Chattaraj, P.K. Conceptual Density Functional Theory based Electronic Structure Principles. *Chem. Sci.* **2021**, *12*, 6264–6279. [[CrossRef](#)]
61. Zhou, K. Theoretical studies on the pentaatomic planar tetracoordinate carbon molecules CGa₃Si and CGa₃Si⁻. *Comput. Theor. Chem.* **2013**, *1009*, 30–34. [[CrossRef](#)]
62. Zubarev, D.Y.; Boldyrev, A.I. Developing Paradigms of Chemical Bonding: Adaptive Natural Density Partitioning. *Phys. Chem. Chem. Phys.* **2008**, *10*, 5207–5217. [[CrossRef](#)]
63. Zubarev, D.Y.; Boldyrev, A.I. Revealing Intuitively Assessable Chemical Bonding Patterns in Organic Aromatic Molecules via Adaptive Natural Density Partitioning. *J. Org. Chem.* **2008**, *73*, 9251–9258. [[CrossRef](#)]
64. von Ragué Schleyer, P.; Jiao, H.; Hommes, N.v.E.; Malkin, V.G.; Malkina, O.L. An Evaluation of the Aromaticity of Inorganic Rings: Refined Evidence from Magnetic Properties. *J. Am. Chem. Soc.* **1997**, *119*, 12669–12670. [[CrossRef](#)]
65. von Ragué Schleyer, P.; Maerker, C.; Dransfeld, A.; Jiao, H.; van Eikema Hommes, N.J.R. Nucleus-Independent Chemical Shifts: A Simple and Efficient Aromaticity Probe. *J. Am. Chem. Soc.* **1996**, *118*, 6317–6318. [[CrossRef](#)] [[PubMed](#)]